Title

Sex-dependent structure of socioemotional salience, executive control, and default mode networks in preschool-aged children with autism

Journal

NeuroImage, 257(Cereb. Cortex 29 2019)

ISSN

1053-8119

Authors

Zielinski, Brandon A

Andrews, Derek S

Lee, Joshua K

et al.

Publication Date

2022-08-01

DOI

10.1016/j.neuroimage.2022.119252

Peer reviewed

HHS Public Access

Author manuscript

Neuroimage. Author manuscript; available in PMC 2024 May 21.

Published in final edited form as:

Neuroimage. 2022 August 15; 257: 119252. doi:10.1016/j.neuroimage.2022.119252.

Sex-dependent structure of socioemotional salience, executive control, and default mode networks in preschool-aged children with autism

Brandon A. Zielinski[a,*] **[Conceptualization]**, **Derek S. Andrews**[b] **[Investigation]**, **Joshua K. Lee**[b] **[Investigation]**, **Marjorie Solomon**[b] **[Resources]**, **Sally J. Rogers**[b] **[Resources]**, **Brianna Heath**[b] **[Data curation]**, **Christine Wu Nordahl**[b] **[Conceptualization]**, **David G. Amaral**[b] **[Conceptualization]**

[a]Departments of Pediatrics and Neurology, University of Utah School of Medicine, University of Utah, Salt Lake City, UT, USA

[b]The Medical Investigation of Neurodevelopmental Disorders (MIND) Institute and Department of Psychiatry and Behavioral Sciences, UC Davis School of Medicine, University of California Davis, Sacramento, CA, USA

Abstract

The structure of large-scale intrinsic connectivity networks is atypical in adolescents diagnosed with autism spectrum disorder (ASD or autism). However, the degree to which alterations occur in younger children, and whether these differences vary by sex, is unknown. We utilized structural magnetic resonance imaging (MRI) data from a sex- and age-matched sample of 122 autistic and 122 typically developing (TD) children (2–4 years old) to investigate differences in underlying network structure in preschool-aged autistic children within three large scale intrinsic connectivity networks implicated in ASD: the Socioemotional Salience, Executive Control, and Default Mode Networks. Utilizing structural covariance MRI (scMRI), we report network-level differences in autistic versus TD children, and further report preliminary findings of sex-dependent differences within network topology.

1. Introduction

Autism spectrum disorder (ASD or autism) is a complex neurodevelopmental diagnosis characterized by childhood onset of alterations in social communication and the presence of repetitive or restricted behaviors (DSM-IV-TR; American Psychiatric Association

*Corresponding author. brandon.zielinski@hsc.utah.edu (B.A. Zielinski).

Disclosures: DGA is on the scientific advisory board for Stemina Biomarker Discovery and Axial Biotherapeutics. All other authors have no competing interests to report.

Credit authorship contribution statement

Brandon A. Zielinski: Methodology, Software, Formal analysis, Writing – original draft, Writing – review & editing, Visualization. **Derek S. Andrews:** Resources, Data curation, Writing – review & editing. **Joshua K. Lee:** Resources, Data curation, Writing – review & editing. **Marjorie Solomon:** Funding acquisition. **Sally J. Rogers:** Funding acquisition. **Brianna Heath:** Project administration. **Christine Wu Nordahl:** Investigation, Resources, Data curation, Writing – review & editing, Funding acquisition, Supervision. **David G. Amaral:** Investigation, Resources, Writing – review & editing, Funding acquisition, Supervision.

Diagnostic and Statistical Manual of Mental Disorders (DSM-4®, 2000). Symptoms are manifest in multiple cognitive domains including socio-emotional function, executive functions such as flexible anticipatory judgment, and processing of internally-versus externally-directed stimuli. Large-scale brain networks have increasingly become implicated in ASD symptomatology, particularly the Socioemotional Salience (SN), Executive Control (ECN), and Default Mode (DMN) networks, which underlie the above cognitive domains, respectively (Seeley et al., 2007; Kennedy et al., 2006, 2008; Sridharan et al., 2008).

Although numerous resting state functional MRI (rsfMRI) studies have characterized large-scale network topology in adults (Fox et al., 2005; Beckmann et al., 2005; Damoiseaux et al., 2006), relatively little work on network structure and function has been carried out in young children. Further, very young children at an age when an autism diagnosis is first clinically reliable (~2,3 years), particularly those with intellectual disabilities, are underrepresented in the literature. This is due to a variety of MRI compliance issues such as holding still, maintaining focus, and tolerating the MRI scanner environment for sustained periods (Nordahl et al., 2008). Imaging techniques that can evaluate network-level structure in both very young and in challenging populations are critical to assessing possible developmental alterations to brain networks. A promising technique to examine large-scale brain network organization is structural covariance MRI (scMRI; Zielinski et al., 2010), which identifies brain regions with co-varying gray matter density across participants, and determines network-specific topology of whole-brain gray matter signal covariance (structural covariance networks; SCNs).

Using scMRI techniques, divergent Salience and Default Mode network alterations have been identified in older autistic children and adolescents (mean age ~13.5 years; range 9–22 yrs) (Zielinski et al., 2012). The overall volume and extent of the SN was substantially reduced in the ASD group, representing only 8% of the SN volume observed in TD controls. Further, multiple hallmark nodes of the SN, such as the anterior cingulate cortex, medial frontal wall and lateral frontal operculum were not apparent in the ASD group. Conversely, the DMN was larger in volume and extent in ASD, and appeared to have an anterior-posterior decoupling, with relative right lateralized overgrowth posteriorly. This work is consistent with more recent studies utilizing public databases (Cai et al., 2021), and has been extended to other networks including speech and language (Sharda et al., 2016), as well as subcortical structures (Duan et al., 2020) implicated in autism. Complementary approaches utilizing distinct measures including cortical thickness (Bethlehem et al., 2017; Valk et al., 2015; Zielinski et al., 2014) and gyrification index (Zoltowski et al., 2021) have also converged on a network-based framework for autism.

The studies cited above, and more general investigations of structure-function relationships across the field, have typically not included preschool-aged children (2–5 years of age), a time of rapid brain development. Thus, where, when, and how network alterations in ASD diverge from typical development is unknown. Early-stage evaluation of the neuroanatomy of autism is critical to understanding real world clinical impacts of therapeutic interventions. Further, sex-dependent differences in intrinsic connectivity network structure in young children are virtually unknown. An emerging literature has identified robust differences between older males and females with autism (Walsh et al., 2021), including within and

between network connectivity of the SN, ECN, and DMN (Alaerts et al., 2016). A recent study from the GENDAAR consortium found sex differences in DMN-ECN connectivity between autistic females and males that are not present in TD and further identified an attenuation of typical sex differences in SN functional connectivity in autism (Lawrence et al., 2020). Evaluation of sex differences in these networks in younger children with autism is currently lacking.

Leveraging a unique age and sex matched cohort of young autistic children and TD controls from the UC Davis MIND Institute Autism Phenome Project (APP), we utilized scMRI to compare network-level structure of the DMN, ECN, and SN in ASD and TD children aged 2–4 years of age. Our primary goal was to compare network alterations of these younger children with those previously identified in older children and adolescents. We first performed qualitative analyses to examine integrity and topology of structural covariance networks in this cohort and to permit comparison to previously characterized intrinsic connectivity networks using scMRI and resting state fMRI. We then performed quantitative between-group analyses to determine specific alterations in network structure that more strongly contributed to network-level differences between diagnostic groups and sex. Finally, we evaluated quantitative, diagnosis-by-sex interactions to determine whether differences in network structure between children with autism and TD controls were influenced by sex.

2. Methods

2.1. Participants

Participants were enrolled in either the UC Davis MIND Institute Autism Phenome Project, Girls with Autism – Imaging of Neurodevelopment (GAIN), or Brain Research in Autism Investigating Neurophenotypes (BRAIN) studies. These associated studies have a shared longitudinal design that includes enrollment, baseline MRI, and behavioral assessment at 2–4 years of age (Time 1) and planned follow up across childhood and adolescence. Participants in the GAIN and BRAIN studies are considered to be part of the APP. The present cross-sectional study included a balanced subset of ASD and TD, male and female participants selected from all participants who successfully completed MRI at Time 1 (Table 1). Balanced samples were achieved using procedures described below. Participants were required to be native English speakers, ambulatory, have no contraindications for MRI, and no known or suspected vision or hearing problems, identified genetic disorders (e.g. Fragile X) or neurodevelopmental conditions.

At Time 1, ASD diagnosis was confirmed using the Autism Diagnostic Observation Schedule-Generic (ADOS-G) (Lord et al., 2000) or ADOS-2 (Lord et al., 2012), the Autism Diagnostic Interview-Revised (ADI-R) (Lord et al., 1994) and DSM-IV-TR criteria (American Psychiatric Association Diagnostic and Statistical Manual of Mental Disorders (DSM-4®), 2000). Non-autistic, non-developmentally delayed children were enrolled as TD controls. TD children were screened for autism traits using the Social Communication Questionnaire (SCQ; Rutter et al., 2003) and had developmental scores within two standard deviations on all sub-scales of the Mullen Scales of Early Learning (MSEL) (Mullen, 1995); they also had no first-degree relatives at the time of enrollment with an ASD diagnosis. The

MSEL was not administered to one TD male who was assessed using the Stanford Binet 5th edition abbreviated IQ battery (Roid, 2003). Informed consent and permission was obtained from the parent or guardian of each participant. All aspects of the study protocol were approved by the University of California Davis Institutional Review Board. For additional details and assessments see supplementary materials.

2.2. MRI scan acquisition

High resolution, T1-weighted structural MRI scans were acquired using 3-dimensional magnetization-prepared rapid acquisition gradient-echo (MPRAGE: TR 2170 ms, TE 4.86 ms, FOV 256, 192 sagittal slices, 1.0 mm slice thickness, 192×256×256 matrix) at the UC Davis Imaging Research Center on a 3T Siemens Trio MRI system using an eight-channel head coil. All scans were acquired during natural, nocturnal sleep (Nordahl et al., 2008). Image distortion associated with changes in software over time was controlled for by scanning a calibration phantom (ADNI MAGPHAM, The Phantom Laboratory) at the end of each MRI session and subsequently applying distortion correction to each image volume (Image Owl, Inc., Greenwich, NY; http://www.imageowl.com).

2.3. Quality control and group assignment

Structural MRI scans were inspected for motion, blurring, artifact, and gross anatomical abnormality including megalencephaly. Participants previously classified as having disproportionate megalencephaly were not included due to evidence that this represents a distinct autism neurophenotype (Ohta et al., 2016; Libero et al., 2016, 2018; Amaral et al., 2017; Lee et al., 2021). After initial scMRI preprocessing was completed (see below), image volumes were again inspected for validity and accuracy of tissue class segmentation and realignment to standardized space. This yielded 272 participant scans. Structural covariance techniques are inherently reliant upon variance embedded in the samples under study. To limit this technical bias introduced by disparate sample sizes, discordant ages, or sex differences, we matched our subgroups as closely as possible on these factors. At the time of analysis, TD females comprised the smallest group ($n = 61$). Thus, this group was constructed initially, and the other groups (ASD males, ASD females, TD males) were subsequently manually matched by age and gender, yielding four matched groups each comprised of 61 participants for a total scMRI sample of 244 individuals.

2.4. Demographics

After matching, ASD and TD groups did not significantly differ ($p > 0.05$, two-tailed t-test) for age of MRI acquisition ($p = 0.99$; see Table 1). Compared to the TD sample, autistic children had significantly lower overall IQ scores ($p < 0.001$). Autistic males did not significantly differ from autistic females in age at MRI acquisition, IQ, ADOS Calibrated Severity Score (CSS), Social Affective-CSS, or Repetitive and Restricted Behavior-CSS scores (Hus et al., 2014; Gotham et al., 2009). TD males did not significantly differ from TD females in age at MRI acquisition. TD females had significantly higher IQ scores than TD males ($t = 2.77$, $p = 0.006$). sc *MRI methods.* We used voxel-based scMRI (Seeley

Supplementary materials
Supplementary material associated with this article can be found, in the online version, at doi: 10.1016/j.neuroimage.2022.119252.

et al., 2009; Zielinski et al., 2010) to interrogate network-level differences in gray matter structure within the SN, ECN, and DMN, three canonical large-scale intrinsic connectivity networks strongly implicated in autism (Menon, 2018). These methods have been described in detail previously (Zielinski et al., 2010, 2012). Briefly, T1 MRI images were realigned, segmented, normalized, modulated, and smoothed using a customized template based on the study sample, as implemented in SPM8 (http://www.fil.ion.ucl.ac.uk/spm). Seed regions-of-interest (ROIs) consisted of 4-mm radius spheres placed within core anatomical hubs of each network (hub; centroid) examined: socio-emotional Salience (anterior frontoinsula cortex, aFI; 38, 24, −11), default mode (posterior cingulate cortex, PCC; 4, −40, 36), and executive-control (dorsolateral prefrontal cortex, DLPFC; 44, 36, 21). Right hemisphere seeds were used for all networks to avoid confounds of language-influenced asymmetries.

Extracted mean ROI gray matter intensities provided covariates-of-interest for whole brain condition (diagnosis or sex)-by-covariate general linear model analyses for each network hub. Total brain volume and age were entered as nuisance covariates. One-sample t-tests were performed to identify voxels with significant group-wise gray matter signal covariance across participants. Resulting seed covariance maps for each diagnostic group were thresholded at $p < 0.01$, family-wise error (FWE) corrected, and displayed on the sample-specific template. These maps were subsequently used to qualitatively compare differences across diagnoses and sex.

To quantify differences in network covariance, direct between-group comparisons of seed covariance between both diagnosis- and sex-based groups ($p < 0.05$, inclusively masked to the network global map for both groups at $p < 0.01$ FWE) were performed using one-tailed t-tests (e.g. ASD > TD; $p < 0.05$). Peak voxel and cluster characteristics were generated using the aal toolbox within SPM8 (http://www.cyceron.fr/web/aal__anatomical_automatic_labeling.html). Age was modeled as a nuisance covariate and resulted in minimal appreciable topological differences in the resulting maps, likely due to sample size and group matching. Lastly, to evaluate possible diagnostic differences associated with sex, a diagnostic group-by-sex interaction term was included in the above model.

3. Results

Qualitative assessment revealed structural covariance network (SCN) topology consistent with prior literature in ASD (Zielinski et al., 2012; Valk et al., 2015; Bethlehem et al., 2017) as well as TD (Zielinski et al., 2010, 2012; see also Evans, 2013, for review). In our TD group, SCNs largely recapitulate rudimentary topology of both structural SCNs (Zielinski et al., 2010) and functional resting state networks (Raichle et al., 2001; Seeley et al., 2007; Beckmann et al., 2005) observed in older children and adults. Similarly, the ASD group largely reflected SCN topology consistent with prior work in older participants (Zielinski et al., 2012). However, qualitative diagnostic group and sex differences in network structure were apparent. In addition, novel findings were demonstrated within networks, which may be due to the younger age and balanced sex (more female subjects) of our sample compared to prior work.

3.1. Network-level structural covariance within ASD and TD

Fig. 1 depicts scMRI maps for the SN, ECN, and DMN in ASD and TD controls (see also Supplemental Table 1). Canonical nodes are represented in the SN, including orbitofrontal cortex and medial frontal cortical wall. In the ECN, classical nodes in TD include ventromedial prefrontal cortex (VMPFC), and dorsal as well as lateral PFC regions. The DMN included anteromedial prefrontal cortex (AMPFC), and to a lesser degree VMPFC, although posterior representation is limited to local covariance surrounding the seed hub and contralateral homologues. In ASD, the SN is spatially restricted when qualitatively compared to TD controls, and also shows robust covariance in bilateral amygdala not observed in TD. Further, regions of covariance outside of the canonical SN, including right primary auditory cortex, are unique to the ASD group. Similarly, the ECN is also spatially restricted in ASD, and shows little covariance outside of seed and contralateral homologous regions. The DMN, however, is expanded posteriorly in ASD, with a right hemisphere extension. Furthermore, frontal nodes seen within TD are not present in ASD at these statistical thresholds.

3.2. Quantitative differences in structural covariance networks between ASD and TD

Quantitative group-wise comparisons revealed a spatially restricted pattern of differences in structural covariance between diagnostic groups. In the SN and ECN, TD covariance was more strongly associated with seed density than in ASD (i.e. One-tailed T-test for TD > ASD (yellow in Fig. 2) and was more robust and widespread than ASD > TD (green)) (Fig. 2 and Supplemental Table 1). Notably, left frontal opercular and orbitofrontal regions were present within the SN of the TD group, whereas only a small region of the right lateral frontal operculum demonstrated covariance in ASD. In the ECN, the ASD group demonstrated significantly greater covariance within discrete clusters in the right DLPFC subjacent to the seed, whereas the TD group had more extensive covariance within a larger cluster superior and lateral to the seed region. As demonstrated in the qualitative comparisons (Fig. 1), DMN covariance was markedly different than SN and ECN, with the ASD group demonstrating highly robust covariance extending laterally from the seed in the posterior cingulate cortex of both hemispheres. Rightward extent was modestly greater compared to left. Only small foci of increased covariance in TD were observed, buried deep within precuneus bilaterally.

3.3. Network-level structural covariance within males and females

The dataset utilized in this study provided sufficient statistical power to investigate sex differences in brain network structure in young children. Qualitatively, we found that each of the studied networks was spatially more distributed in girls than in boys (combined ASD and TD) at this age. Despite similar volumes, topology of the SN and ECN was markedly different between the sexes, with males demonstrating contiguous covariance predominantly frontally compared to females, whose covariance emerged in discrete canonical nodes separated by long distances (Fig. 3 and Supplemental Table 1).

Sex differences were most notable in the DMN, where boys showed little covariance outside of the posterior cingulate cortex hub and contralateral homolog, whereas girls had covariance in multiple discrete posterior, as well as anterior, DMN regions. Girls also had

DMN covariance in the fusiform gyrus, an area in the ‘visual-what’ pathway involved in object recognition (see Grill-Spector and Malach, 2004, for review).

3.4. Quantitative differences in structural covariance networks between males and females

Quantitative group-wise comparisons revealed a more restricted pattern of covariance between boys and girls. However, sex-dependent SCN topology was more variable than seen between diagnostic groups (i.e., ASD v TD). In the SN, only males demonstrated greater covariance (Fig. 4 and Supplemental Table 1). These clusters were in both canonical SCN nodes, including right lateral prefrontal cortex and right anterior frontoinsula cortex, as well as nodes outside of mature adult SN (Seeley et al., 2007, 2019), including right inferior frontal gyrus (the right-sided homolog of Broca’s speech production area), as well as motor system regions of the basal ganglia. Greater ECN covariance was seen in both groups, albeit in disparate regions. Males had stronger covariance in multiple discrete regions of right fontal and prefrontal cortex, in addition to right anterior frontoinsula, typically considered a node within SN. Females, in contrast, covaried more strongly in a discrete focus within left middle frontal cortex. Divergent patterns of covariance were also observed for the DMN, with females having significantly greater covariance in contralateral posterior cingulate cortex and precuneus, whereas males demonstrated greater covariance within a single cluster in pericallosal cortex juxtaposed to the splenium of the corpus callosum.

3.5. Interactions of sex and diagnosis

Significant diagnosis-by-sex interactions in structural covariance were observed in focal regions within canonical SCNs, although some unexpected nodes were outside of classical network boundaries (Fig. 5 and Supplemental Fig. 1). In the SN, significant diagnosis-by-sex interactions in covariance were seen in bilateral frontal opercular, right lateral prefrontal, and left orbitofrontal cortices, overlapping with regions of greater covariance seen in ASD and TDC in the direct group contrast depicted in Fig. 2 and within the group-level SCNs depicted in Fig. 1. ASD males had greater covariance compared to TD males, whereas ASD females had decreased covariance compared to TD. In the ECN, multiple discrete clusters were observed in right prefrontal regions, including right middle frontal (medially and laterally), right inferior frontal (laterally), and anterior frontal cortex. Here again, ASD males had greater covariance compared to TD males, whereas ASD females had decreased covariance compared to TD. In the DMN, significant interaction effects were limited to a single discrete node within left paracentral posterior cingulate cortex, which was nearly wholly encompassed by the large cluster of increased covariance observed in ASD in Fig. 2 and within the group-level SCNs depicted in Figs. 1 and 3. ASD males had greater covariance compared to TD males, whereas ASD and TD females had similar structural covariance. In general, the interaction plots consistently exhibit an interaction pattern reflecting strongest covariance in ASD males and TD females.

4. Discussion

4.1. Atypical network structure in ASD

Utilizing an age- and sex-matched cohort of young children with autism and TD controls, this study aimed to evaluate differences associated with ASD and biological sex in intrinsic connectivity network structure for three well-established large-scale brain networks; Socioemotional Salience (SN), Executive Control (ECN), and Default Mode (DMN). A related goal was to determine if alterations in network organization were similar to those previously reported in older autistic individuals (Zielinski et al., 2012; Valk et al., 2015; Bethlehem et al., 2017). Within ASD, the SN and ECN were observed to be reduced in volume and contain regions with significantly reduced structural covariance compared to TD controls. Conversely, the DMN was found to be increased in volume and have significantly greater structural covariance in ASD compared to TD controls. Significant sex-by-diagnosis effects were observed within regions of all three networks, and were consistently marked by a pattern of ASD males having greater covariance compared to TD males, whereas ASD females had decreased covariance compared to TD females. The current study provides evidence that autistic children between the ages of 2 and 4 years have both qualitative and quantitative differences in large-scale brain network architecture compared to typically developing peers and highlights biological sex as an important mediator of these effects. Network topology was generally consistent with prior work in older children and adolescents (Zielinski et al., 2010, 2012; Valk et al., 2015; Bethlehem et al., 2017; Evans, 2013).

The SN is anchored by the right anterior frontoinsula cortex and supports socioemotional functions (Seeley et al., 2007, 2019). Consistent with prior work, we found the SN is markedly reduced in size and has an atypical distribution in ASD. Notably, brain regions outside of classical SN, but long-implicated in the pathophysiology of autism, including the transverse gyrus of Heschl (Prigge et al., 2013), the functional home of primary auditory cortex, as well as bilateral amygdala, demonstrated covariance with right anterior frontoinsula cortex in ASD but not in TD. Importantly, this qualitative finding replicates prior work in an independent dataset comprised of older children and adolescents (Zielinski et al., 2012). Recognizing that autistic individuals often exhibit profound emotional responses to seemingly innocuous auditory stimuli (Carson et al., 2021), the need to relate this network structure to measured auditory function in the context of emotion is clear. Future work may determine whether atypical coupling between socio-emotional brain regions and acoustic processing regions persist throughout autistic development. In addition, the link between accelerated amygdalar growth and development in autism (Nordahl et al., 2012) as well as postmortem tissue analyses describing increased axonal spine density in younger autistic subjects (Weir et al., 2012) requires further study in the context of socioemotional function at this age. Statistically significant differences at these thresholds reflected hemispheric asymmetries between ASD and TD nodes, and these clusters were contained within qualitative maps as described above.

The ECN, sometimes referred to as the central executive, or fronto-parietal network, is implicated in supporting working memory and fluid intelligence. This network is responsible

for anticipatory judgment and flexible, goal-directed actions, among other functions, and consistent with SN, is reduced in volume and extent in autism at this age. Despite involvement of canonical ECN nodes such as ventromedial prefrontal cortex and anterior cingulate cortex observed in the TD group, we found the ASD group had little covariance outside of contralateral dorsolateral prefrontal cortex. Longitudinal analyses are needed to determine whether this represents a delay of network development, or a redistribution of a central network hub (i.e. ECN anchor outside of DLPFC). As seen in the SN, statistically significant quantitative differences between ASD and TD groups in ECN covariance were contained within the qualitative maps.

The most widely studied intrinsic connectivity network is the DMN. The principal function of this network is thought to be directing attention, such that when salient stimuli are perceived, the DMN disengages, permitting or even directing connectivity in or between other networks to emerge (Uddin and Menon 2009). Replicating prior reports (Zielinski et al., 2012), we found that DMN covariance, in contrast to the SN and ECN, has greater volume in ASD than TD, does not exhibit the anterior covariance seen in TD, and has a right lateralized predominance posteriorly. This ‘overgrown’, right-dominant ‘posteriorization’, or anterior-posterior decoupling, may thus be a fundamentally significant finding in young autistic individuals that persists throughout early development. Given the principal importance of the DMN, and support from rsfMRI studies implicating posterior cingulate cortex and right paramedian parietal regions in ASD (Lau et al., 2019), further study of this finding in the context of DMN development across childhood may yield important clues to the pathophysiology, as well as therapeutic targets, of autism.

4.2. Sex-dependent differences

Sex specific divergence in structural brain network architecture in young children has not previously been detailed. In the SN, canonical nodes including orbitofrontal cortex and regions along the medial frontal wall were qualitatively observed in girls. Whereas in boys, co-variance was limited to contralateral homologues and locally expanded right frontal opercular covariance. In addition, only boys had extensive covariance in the basal ganglia, particularly within bilateral putamen, typically considered a major relay pathway in the motor system. Involvement of the putamen in ASD has been described previously (Postema et al., 2019.) Notably, only males showed significantly increased covariance, seen within right anterior frontoinsula, putamen, and ventrolateral prefrontal cortex.

The ECN, qualitatively, had frontally expanded covariance in boys, whereas girls demonstrated involvement of posterior nodes including some regions typically considered DMN nodes, such as the posterior cingulate cortex. Whether this suggests delayed development of frontal network architecture or segregation in girls, or early cross-network integration, remains uncertain. Further work in this age group may determine whether boys first develop action-decision circuitry in frontal regions, whereas girls first develop social brain regions, in the context of emotion. Direct statistical comparisons revealed regions of increased structural covariance in frontal, opercular, frontopolar, and insular clusters in males, and a single cluster in left middle frontal cortex in females.

Within the DMN, boys qualitatively demonstrated little covariance outside of the right posterior cingulate cortex hub and its left hemisphere homolog, whereas girls showed sparse but appreciable covariance in widely distributed regions within the mature, adult DMN. Moreover, girls also demonstrated covariance in the fusiform gyrus, including a subregion specialized for perception of human faces (Kanwisher and Yovel, 2006). As these regions were not statistically different at these thresholds, it is premature to conclude that girls may be more attuned to human faces as important stimuli in need of attention. However, given the function of the DMN in stimulus filtering, further investigating the relationship of human face perception to DMN structure and function in this age group is intriguing. Direct comparisons revealed increased covariance within bilateral posterior cingulate cortex and surrounding regions in females, whereas males demonstrated a single cluster of increased covariance in pericallosal cortex of the right hemisphere.

Importantly, across all three networks we observed clusters of significant sex-by-diagnosis interaction effects. These effects revealed a consistent pattern of autistic males having greater covariance compared to TD males, whereas autistic females had decreased covariance compared to TD females. Although scMRI studies of sex-effects in ASD are sparse, previous work using functional connectivity MRI supports this concept, although particular differences have varied between brain regions and between studies (Alaerts et al., 2016; Lee et al., 2020). While the effect of biological sex on network architecture in ASD requires more study, taken together these studies suggest males and females with autism regularly differ from their sex-matched counter-parts in different ways, suggesting that there exist both qualitative and quantitative differences in how autism manifests in males and females (Hammill et al., 2021).

It should be underscored that our findings reflect sex differences in a sex-balanced group of males with and without autism compared to females with and without autism. Although we report sex-by-diagnosis interactions, namely in right lateral frontal operculum (SN), right lateral and medial prefrontal cortex (ECN), and left posterior cingulate cortex (DMN), our data would benefit from increased power to comprehensively examine these four subgroups independently, ideally with larger samples and extensive neurobehavioral measures. Similarly, although many of the qualitative differences reported here did not reach statistical significance in our direct quantitative comparisons, these findings may prove robust when employing larger samples or less conservative thresholds than those used here. Future research, both longitudinal, as well as sufficiently powered to examine both ASD as well as TD boys and girls separately, is critical to clarify our findings and to identify novel relationships between SCN architecture and neurobehavioral data. Whether differences associated with autism or sex reported here extend to other intrinsic connectivity networks is an area of ongoing investigation.

While the young age and well-matched sample are significant strengths of this study, it is important to note several limitations. The precise signal source underlying scMRI remains elusive. Studies are underway to clarify the relative contributions of microscopic gray matter and white matter, and other biological material that forms the basis of T1-weighted MRI gray matter signal intensity. However, this consideration is not new, and has been debated clinically despite the impact of MRI in medicine. Our study utilizes standard clinical T1-

weighted MRI sequences and is not constrained by anatomic labels, regional boundaries which may vary by subject, or other technical issues which impact alternative structural methods (such as detecting pial surface boundaries). However, future studies may benefit from multimodal methodologies including cortical surface-based morphometry approaches to cross-validate current findings with measures such as cortical thickness and surface area. Further, in contrast to resting state fMRI, scMRI is not likely impacted by sleep state, enabling use of this technique in our young sample. Here again, future studies in older awake individuals combining functional connectivity with structural covariance may provide insight into functional network dynamics related to our observed findings. Lastly, in this initial analysis we report scMRI topologies in very young children with and without ASD, drawing parallels between this and previous work employing similar techniques and data processing strategies, and providing a framework for future studies of sex-dependent differences in ASD and in child development. Future work will examine in greater detail neurobehavioral assessment, cognitive capability, and developmental stage in the context of functional and structural network neurobiology.

5. Conclusion

We report sex-dependent differences in structural covariance network topology in young children with autism compared to age and sex matched typically-developing children. Consistent with prior reports, we found that the SN, ECN, and DMN are relatively underdeveloped in early childhood compared to canonical adult networks, although the main hubs and nodes are represented to varying degrees. This underscores the well-known developmental ontogeny of brain compartments, volumes, and tissues, but here further extends prior work to the level of the large-scale brain network in younger children. Our findings support the conclusion that autism is associated with atypical network structure in young children, and that at least some of these atypicalities are influenced by biological sex. Our work highlights that network architecture in ASD is not uniformly divergent from TD, but may show network specificity in atypical distribution and extent, here again which may be influenced by sex. Lastly, this and other studies of network structure are cross-sectional. Longitudinal studies with larger samples are critically needed to detail both individual and group trajectories of network development.

Supplementary Material

Refer to Web version on PubMed Central for supplementary material.

Acknowledgments

The authors would like to thank the families and children who participated in the APP study and all members of the research study staff. This research was supported by an Autism Center of Excellence grant awarded by the National Institute of Child Health and Development (NICHD) (P50 HD093079) as well as the National Institute of Mental Health (R01MH104438 [CWN], R01MH103284 [MS], R01MH103371 [DGA], K08MH100609 [BAZ]). DSA was supported by the MIND Institute Autism Research Training Program (T32MH073124).

References

Alaerts K, Swinnen SP, Wenderoth N, 2016. Sex differences in autism: a resting-state fMRI investigation of functional brain connectivity in males and females. Soc. Cognit. Affect. Neurosci. 11, 1002–1016. [PubMed: 26989195]

Amaral DG, Li D, Libero L, Solomon M, Van de Water J, Mastergeorge A, Naigles L, Rogers S, Wu Nordahl C, 2017. In pursuit of neurophenotypes: the consequences of having autism and a big brain. Autism Res. 10, 711–722. [PubMed: 28239961]

American Psychiatric Association Diagnostic and Statistical Manual of Mental Disorders (DSM-4®). 2000. American Psychiatric Publishing. 1994.

Beckmann CF, DeLuca M, Devlin JT, Smith SM, 2005. Investigations into resting-state connectivity using independent component analysis. 2005. Philos. Trans. R. Soc. B Biol. Sci. 360, 1001–1013.

Bethlehem RAI, Romero-Garcia R, Mak E, Bullmore ET, Baron-Cohen S, 2017. Structural covariance networks in children with autism or ADHD. Cereb. Cortex 27, 4267–4276. [PubMed: 28633299]

Cai S, Wang X, Yang F, Chen D, Huang L, 2021. Differences in brain structural covariance network characteristics in children and adults with autism spectrum disorder. Autism Res. 14, 265–275. [PubMed: 33386783]

Carson TB, Valente MJ, Wilkes BJ, Richard L, 2021. Brief report: prevalence and severity of auditory sensory over-responsivity in autism as reported by parents and caregivers. J. Autism Dev. Disord. 52, 1395–1402. [PubMed: 33837888]

Damoiseaux JS, Rombouts SA, Barkhof F, Scheltens P, Stam CJ, Smith SM, Beckmann CF, 2006. Consistent resting-state networks across healthy subjects. Proc. Natl. Acad. Sci. 103, 13848–13853. [PubMed: 16945915]

Duan X, Wang R, Xiao J, Li Y, Huang X, Guo X, Cao J, He L, He C, Ling Z, Shan X, Chen H, Kang X, Chen H, 2020. Subcortical structural covariance in young children with autism spectrum disorder. Prog. Neuropsychopharmacol. Biol. Psychiatry 99, 109874.

Evans AC, 2013. Networks of anatomical covariance. Neuroimage 80, 489–504. [PubMed: 23711536]

Fox MD, Snyder AZ, Vincent JL, Corbetta M, Van Essen DC, Raichle M, 2005. The human brain is intrinsically organized into dynamic, anticorrelated functional networks. Proc. Natl. Acad. Sci. 102, 9673–9678. [PubMed: 15976020]

Grill-Spector K, Malach R, 2004. The human visual cortex. Ann. Rev. Neurosci. 27, 649–677. [PubMed: 15217346]

Hammill C, Lerch JP, Taylor MJ, Ameis SH, Chakravarty MM, Szatmari P, Anagnostou E, Lai MC, 2021. Quantitative and qualitative sex modulations in the brain anatomy of autism. Biol. Psychiatry Cognit. Neurosci. Neuroimaging 6, 898– 909. [PubMed: 33713843]

Hus V, Gotham K, Lord C, 2014. Standardizing ADOS domain scores: separating severity of social affect and restricted and repetitive behaviors. J. Autism Dev. Disord. 44, 2400–2412. [PubMed: 23143131]

Kanwisher N, Yovel G, 2006. The fusiform face area: a cortical region specialized for the perception of faces. Philos. Trans. R. Soc. B Biol. Sci. 361, 2109–2128.

Kennedy DP, Redcay E, Courchesne E, 2006. Failing to deactivate: resting functional abnormalities in autism. Proc. Natl. Acad. Sci. 103, 8275–8280. [PubMed: 16702548]

Kennedy DP, Courchesne E, 2008. Functional abnormalities of the default network during self-and other-reflection in autism. Soc. Cogn. Affect. Neurosci. 3, 177– 190. [PubMed: 19015108]

Lau WKW, Leung MK, Lau BWM, 2019. Resting-state abnormalities in autism spectrum disorders: a meta-analysis. Sci. Rep. 9, 3892. [PubMed: 30846796]

Gotham K, Pickles A, Lord C, 2009. Standardizing ADOS scores for a measure of severity in autism spectrum disorders. J. Autism Dev. Disord. 39, 693–705. [PubMed: 19082876]

Lawrence KE, Hernandez LM, Bowman HC, Padgaonkar NT, Fuster E, Jack A, Aylward E, Gaab N, Van Horn JD, Bernier RA, Geschwind DH, McPartland JC, Nelson CA, Webb SJ, Pelphrey KA, Green SA, Bookheimer SY, Dapretto M, 2020. Sex differences in functional connectivity of the salience, default mode, and central executive networks in youth with ASD. Cereb. Cortex 30, 5107–5120. [PubMed: 32350530]

Lee JK, Amaral DG, Solomon M, Rogers SJ, Ozonoff S, Nordahl CW, 2020. Sex differences in the amygdala resting-state connectome of children with autism spectrum disorder. Biol. Psychiatry Cognit. Neurosci. Neuroimaging. 5, 320–329 2020. [PubMed: 31563470]

Lee JK, Andrews DS, Ozonoff S, Solomon M, Rogers S, Amaral DG, Nordahl CW, 2021. Longitudinal evaluation of cerebral growth across childhood in boys and girls with autism spectrum disorder. Biol. Psychiatry 90, 286–294. [PubMed: 33388135]

Libero LE, Nordahl CW, Li DD, Ferrer E, Rogers SJ, Amaral DG, 2016. Persistence of megalencephaly in a subgroup of young boys with autism spectrum disorder. Autism Res. 9, 1169–1182. [PubMed: 27273931]

Lord C, Risi S, Lambrecht L, Cook EH, Leventhal BL, DiLavore PC, Rutter M, 2000. The autism diagnostic observation schedule-generic: a standard measure of social and communication deficits associated with the spectrum of autism. J. Autism Dev. Disord. 30, 205–223. [PubMed: 11055457]

Lord C, Rutter M, Le Couteur A, 1994. Autism diagnostic interview-revised: a revised version of a diagnostic interview for caregivers of individuals with possible pervasive developmental disorders. J. Autism Dev. Disord. 24, 659–685. [PubMed: 7814313]

Lord C, Rutter M, DiLavore P, Risi S, Gotham K, Bishop S, 2012. Autism diagnostic observation schedule–2nd edition (ADOS-2). West. Psychol. Corp..

Menon V, 2018. The triple network model, insight, and large-scale brain organization in autism. Biol. Psychiatry 84, 236–238. [PubMed: 30071947]

Mullen EM, 1995. Mullen Scales of Early Learning. AGS Publishing.

Nordahl CW, Simon TJ, Zierhut C, Solomon M, Rogers SJ, Amaral DG, 2008. Brief report: methods for acquiring structural MRI data in very young children with autism without the use of sedation. J. Autism Dev. Disord. 38, 1581–1590. [PubMed: 18157624]

Nordahl CW, Scholz R, Yang X, Buonocore MH, Simon T, Rogers S, Amaral DG, 2012. Increased rate of amygdala growth in children aged 2 to 4 years with autism spectrum disorders: a longitudinal study. Arch. Gen. Psychiatry 69, 53–61. [PubMed: 22213789]

Ohta H, Nordahl CW, Iosif AM, Lee A, Rogers S, Amaral DG, 2016. Increased surface area, but not cortical thickness, in a subset of young boys with autism spectrum disorder. Autism Res. 9, 232–248. [PubMed: 26184828]

Postema MC, van Rooij D, Anagnostou E, Arango C, Auzias G, Behrmann M, Filho GB, Calderoni S, Calvo R, Daly E, Deruelle C, Di Martino A, Dinstein I, Duran FLS, Durston S, Ecker C, Ehrlich S, Fair D, Fedor J, Feng X, Fitzgerald J, Floris DL, Freitag CM, Gallagher L, Glahn DC, Gori I, Haar S, Hoekstra L, Jahanshad N, Jalbrzikowski M, Janssen J, King JA, Kong XZ, Lazaro L, Lerch JP, Luna B, Martinho MM, McGrath J, Medland SE, Muratori F, Murphy CM, Murphy DGM, O'Hearn K, Oranje B, Parellada M, Puig O, Retico A, Rosa P, Rubia K, Shook D, Taylor MJ, Tosetti M, Wallace GL, Zhou F, Thompson PM, Fisher SE, Buitelaar JK, Francks C, 2019. Altered structural brain asymmetry in autism spectrum disorder in a study of 54 datasets. Nat. Commun. 10, 1–12. [PubMed: 30602773]

Prigge MD, Bigler ED, Fletcher PT, Zielinski BA, Ravichandran C, Anderson J, Froehlich A, Abildskov T, Papadopolous E, Maasberg K, Nielsen JA, Alexander AL, Lange N, Lainhart J, 2013. Longitudinal Heschl's gyrus growth during childhood and adolescence in typical development and autism. Autism Res. 6, 78–90. [PubMed: 23436773]

Raichle ME, MacLeod AM, Snyder AZ, Powers WJ, Gusnard DA, Shulman GL, 2001. A default mode of brain function. Proc. Natl. Acad. Sci. 98, 676–682. [PubMed: 11209064]

Rutter M, Bailey A, Lord C, 2003. The social communication questionnaire. West. Psychol. Serv.

Seeley WW, Menon V, Schatzberg AF, Keller J, Glover GH, Kenna H, Reiss A, Greicius M, 2007. Dissociable intrinsic connectivity networks for Salience processing and executive control. J. Neurosci. 27, 2349–2356. [PubMed: 17329432]

Seeley WW, Crawford RK, Zhou J, Miller BL, Greicius MD, 2009. Neurodegenerative diseases target large-scale human brain networks. Neuron 62, 42–52. [PubMed: 19376066]

Seeley WW, 2019. The Salience network: a neural system for perceiving and responding to homeostatic demands. J. Neurosci. 39, 9878–9882. [PubMed: 31676604]

Sharda M, Khundrakpam BS, Evans AC, Singh NC, 2016. Disruption of structural covariance networks for language in autism is modulated by verbal ability. Brain Struct. Funct. 221, 1017–1032. [PubMed: 25445842]

Sridharan D, Levitin DJ, Menon V, 2008. A critical role for the right fronto-insular cortex in switching between central-executive and default-mode networks. Proc. Natl. Acad. Sci. 105, 12569–12574. [PubMed: 18723676]

Uddin LQ, Menon V, 2009. The anterior insula in autism: under-connected and under- -examined. Neurosci. Biobehav. Rev. 33, 1198–1203. [PubMed: 19538989]

Valk SL, Di Martino A, Milham MP, Bernhardt BC, 2015. Multicenter mapping of structural network alterations in autism. Hum. Brain Mapp. 36, 2364–2373. [PubMed: 25727858]

Walsh MJM, Wallace GL, Gallegos SM, Braden BB, 2021. Brain-based sex differences in autism spectrum disorder across the lifespan: a systematic review of structural MRI, fMRI, and DTI findings. Neuroimage Clin. 31, 102719.

Zielinski BA, Gennatas ED, Zhou J, Seeley WW, 2010. Network-level structural covariance in the developing brain. Proc. Natl. Acad. Sci. 107, 18191–18196. [PubMed: 20921389]

Zielinski BA, Anderson JS, Froehlich AL, Prigge MB, Nielsen JA, Cooperrider JR, Cariello AN, Fletcher PT, Alexander AL, Lange N, Bigler ED, Lainhart JE, 2012. scMRI reveals large-scale brain network abnormalities in autism. PLoS One 7, e49172. [PubMed: 23185305]

Zielinski BA, Prigge MB, Nielsen JA, Froehlich AL, Abildskov TJ, Anderson JS, Fletcher PT, Zygmunt KM, Travers BG, Lange N, Alexander AL, Bigler ED, Lainhart JE, 2014. Longitudinal changes in cortical thickness in autism and typical development. Brain 137, 1799–1812. [PubMed: 24755274]

Zoltowski AR, Lyu I, Failla M, Mash LE, Dunham K, Feldman JI, Woynaroski TG, Wallace MT, Barquero LA, Nguyen TQ, Cutting LE, Kang H, Landman BA, Cascio CJ, 2021. Cortical morphology in autism: findings from a cortical shape-adaptive approach to local gyrification indexing. Cereb. Cortex 31, 5188–5205. [PubMed: 34195789]

Further reading

Libero LE, Schaer M, Li DD, Amaral DG, Nordahl CW, 2019. A longitudinal study of local gyrification index in young boys with autism spectrum disorder. Cereb. Cortex 29, 2575–2587. [PubMed: 29850803]

Roid GH, Pomplun M, 2012. The stanford-binet intelligence scales, fifth edition. In: Contemporary Intellectual Assessment: Theories, Tests, and Issues. The Guilford Press, pp. 249–268.

Weir RK, Bauman MD, Jacobs B, Schumann CM, 2018. Protracted dendritic growth in the typically developing human amygdala and increased spine density in young ASD brains. J. Comp. Neurol. 526, 262–274. [PubMed: 28929566]

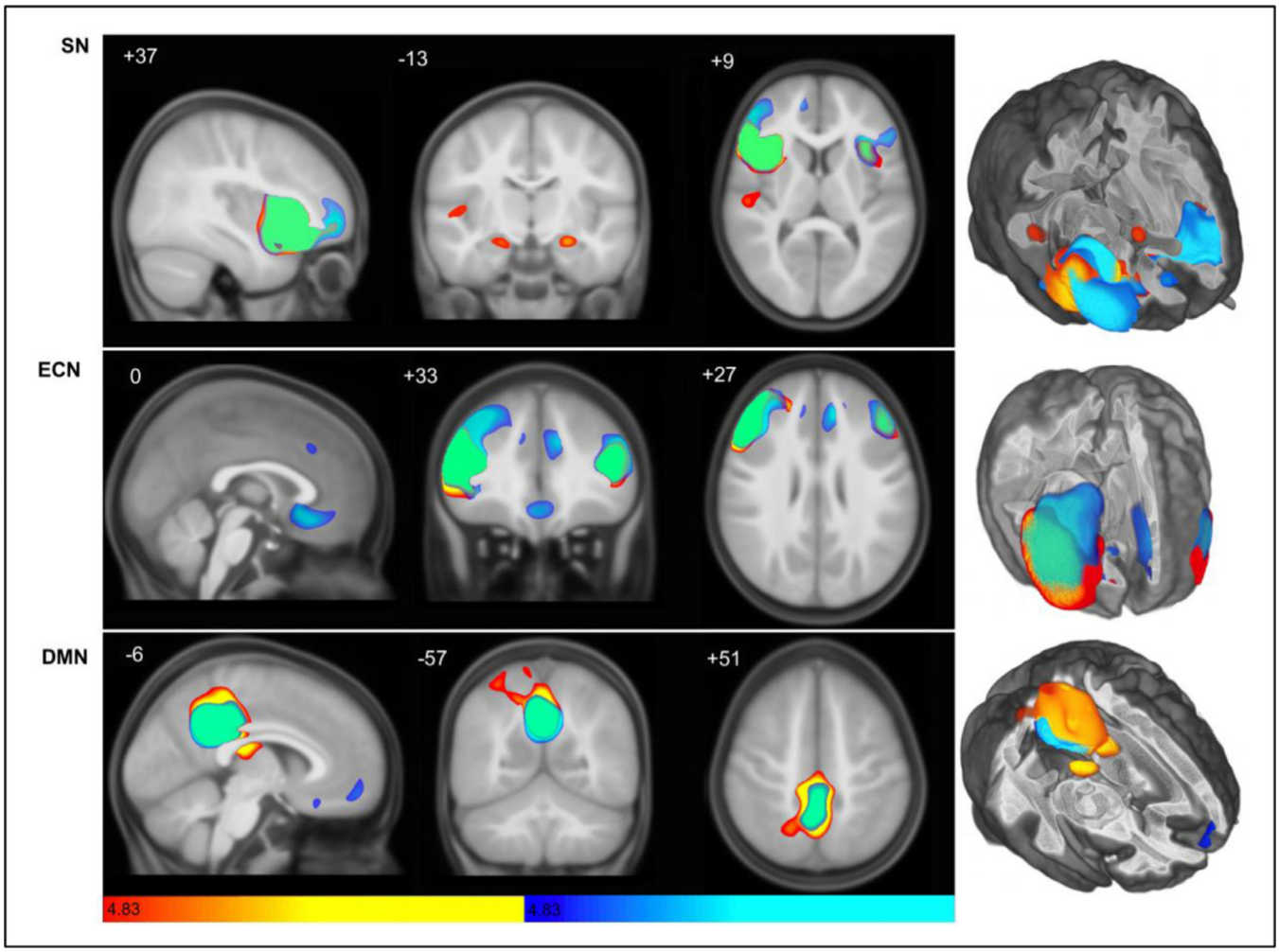

Fig. 1. Structural covariance map of the Salience, executive-control, and default mode networks in autistic and control participants.

Statistical parametric maps depict brain regions in which gray matter intensity covaried with that of the seed ROI in each network in ASD (hot colors) and TD (cool colors). (Top) Salience Network (aFI seed) covariance patterns appear spatially restricted in autism (hot colors; see also Supplemental Table 1), with less frontal covariance as compared to TD, but note involvement of right primary auditory cortex and bilateral amygdala. (Middle) Executive-Control Network (DLPFC seed) scMRI map in TD controls (cool colors; see also Supplemental Table 1) corresponds to a robust canonical ECN, whereas ASD shows very little covariance outside of homologous nodes. (Bottom) scMRI maps of Default Mode Network (PCC seed) demonstrate anterior-posterior decoupling in ASD versus TD, in addition to posterior overgrowth with rightward shift. scMRI data are T-statistic maps ($p < 0.01$, FWE-corrected) displayed on the average anatomical template of all subjects. The left side of the image corresponds to the right side of the brain. $n = 122$ per group. FWE, family-wise error; ROI, region of interest; scMRI, structural covariance MRI.

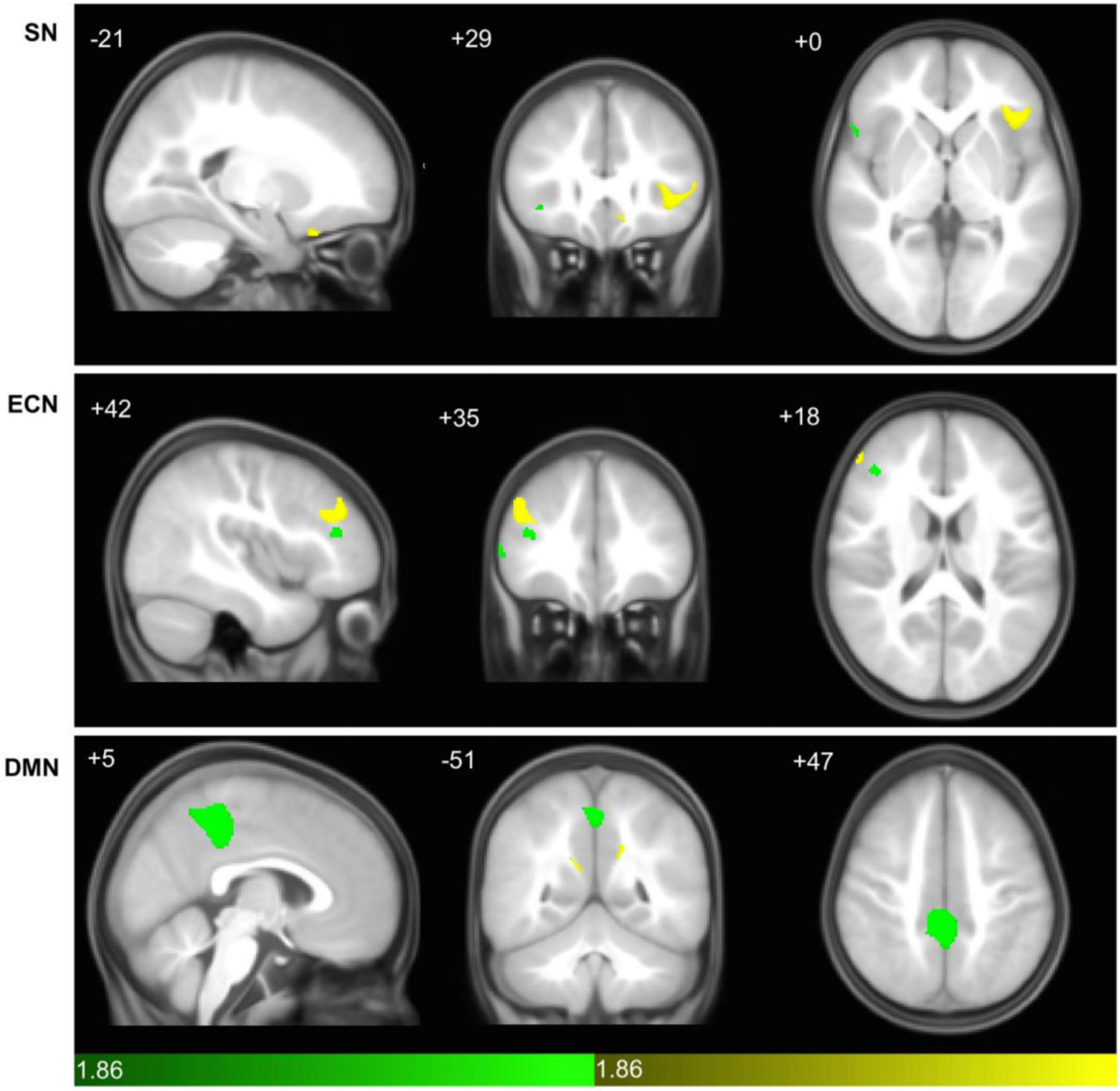

Fig. 2. Direct groupwise contrasts in Salience, executive-control, and default mode networks in autistic and TD control participants.

Statistical parametric maps depict brain regions in which gray matter intensity covaried more strongly with that of the seed ROI in ASD (green) or TD (yellow) in each network. (Top) Salience Network covariance patterns reveal TD contributing more strongly in left frontal operculum and orbitofrontal cortex, whereas ASD had strong covariance in a discrete region of right frontal cortex (see also Supplemental Table 1). (Middle) DLPFC covariance in ASD was strongest in discrete foci subjacent to the seed, whereas in TD a strong cluster superior and lateral to the seed was seen. (Bottom) In the Default Mode Network, bilateral nodes in posterior regions extending laterally from the seed covaried robustly in ASD,

versus discrete foci deep within precuneus in TD. scMRI data are T-statistic maps ($p < 0.05$, of direct groupwise SCNs at $p < 0.01$ FWE-corrected) displayed on the average anatomical template of all subjects. The left side of the image corresponds to the right side of the brain. $n = 122$ per group. FWE, family-wise error; ROI, region of interest; scMRI, structural covariance MRI; DLPFC, dorsolateral prefrontal cortex.

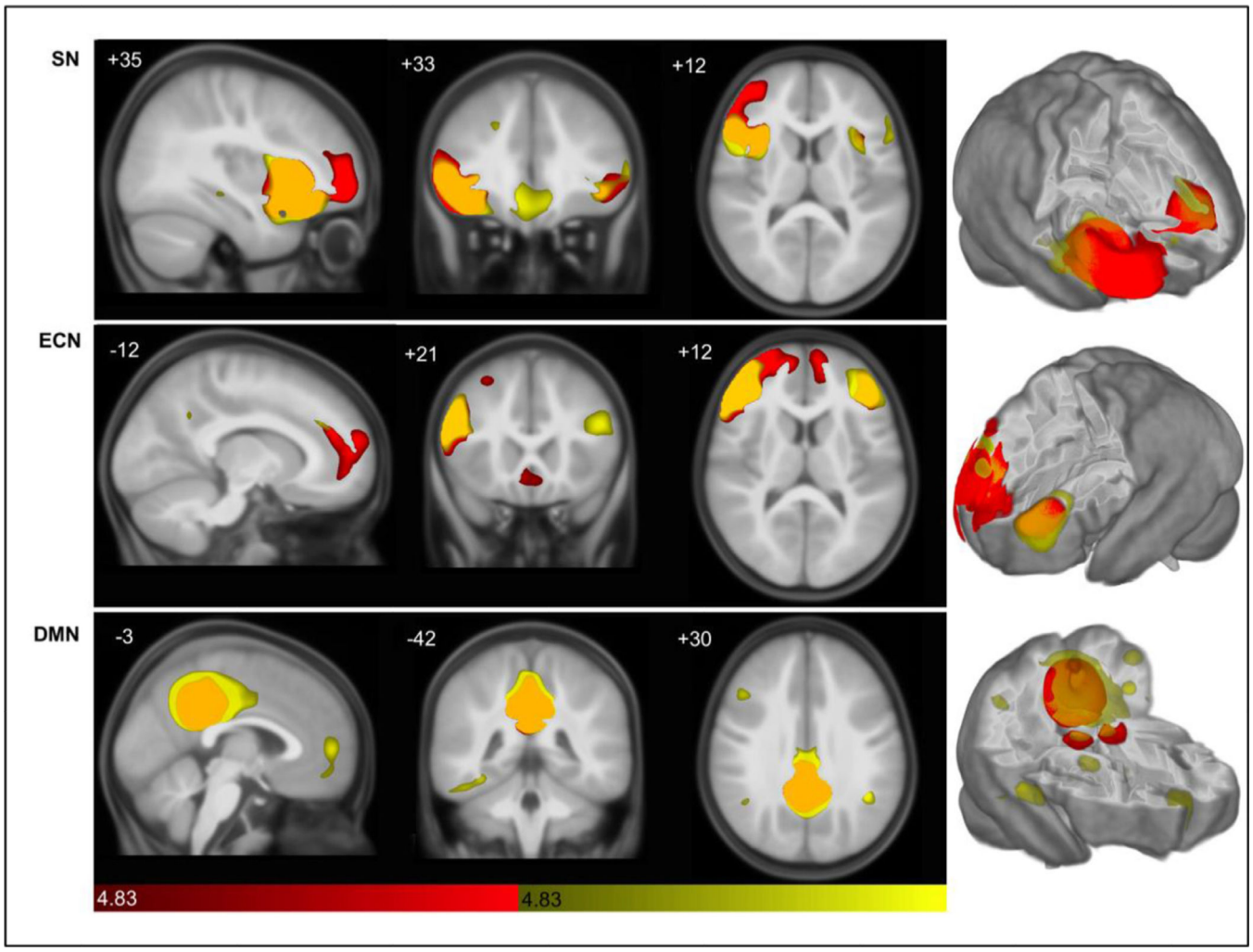

Fig. 3. Structural covariance map of the Salience, executive-control, and default mode networks in males and females.

Statistical parametric maps depict brain regions in which gray matter intensity covaried with that of the seed ROI in each network in males (red) and females (yellow; common regions depicted in orange). (Top) Salience Network covariance patterns appear more spatially distributed in females (see also Supplemental Table 1), with greater locally extensive frontal covariance seen in males. (Middle) Executive-Control Network scMRI map in females again reflects greater spatial distribution, whereas males show frontal midline extension. (Bottom) scMRI maps of Default Mode Network again demonstrate greater anterior-posterior distribution in females, versus little covariance in males. scMRI data are T-statistic maps ($p < 0.01$, FWE-corrected) displayed on the average anatomical template of all subjects. The left side of the image corresponds to the right side of the brain. $n = 122$ per group. FWE, family-wise error; ROI, region of interest; scMRI, structural covariance MRI.

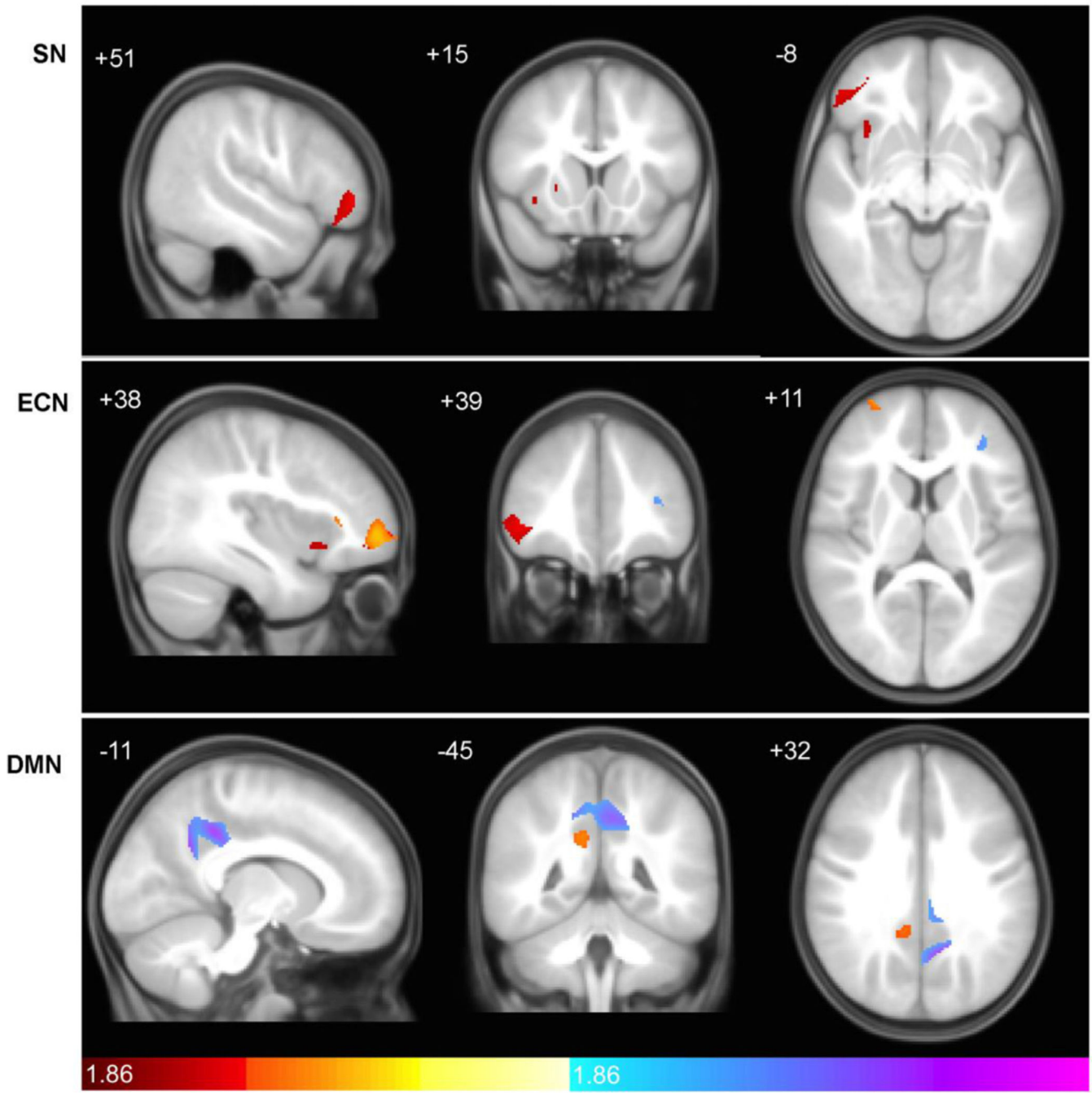

Fig. 4. Direct groupwise contrasts in Salience, executive-control, and default mode networks in males and females.

Statistical parametric maps depict brain regions in which gray matter intensity covaried more strongly with that of the seed ROI in males (hot colors) or females (cool colors) in each network. (Top) Salience Network covariance patterns reveal males contributing more strongly in right frontal and insular cortex, in addition to basal ganglia, whereas females did not covary significantly greater than males in any region (see also Supplemental Table 1). (Middle) DLPFC covariance in males was strongest in multiple regions of frontal, opercular, frontopolar, and insular cortex, whereas in females a modest cluster was evidenced in

contralateral middle frontal cortex. (Bottom) In the Default Mode Network, a node in posterior pericallosal cortex covaried robustly in males, versus robust foci within bilateral but predominantly left PCC and precuneus in females. scMRI data are T-statistic maps ($p < 0.05$, of direct groupwise SCNs at $p < 0.01$ FWE-corrected) displayed on the average anatomical template of all subjects. The left side of the image corresponds to the right side of the brain. $n = 122$ per group. FWE, family-wise error; ROI, region of interest; scMRI, structural covariance MRI; PCC, posterior cingulate cortex; DLPFC, dorsolateral prefrontal cortex.

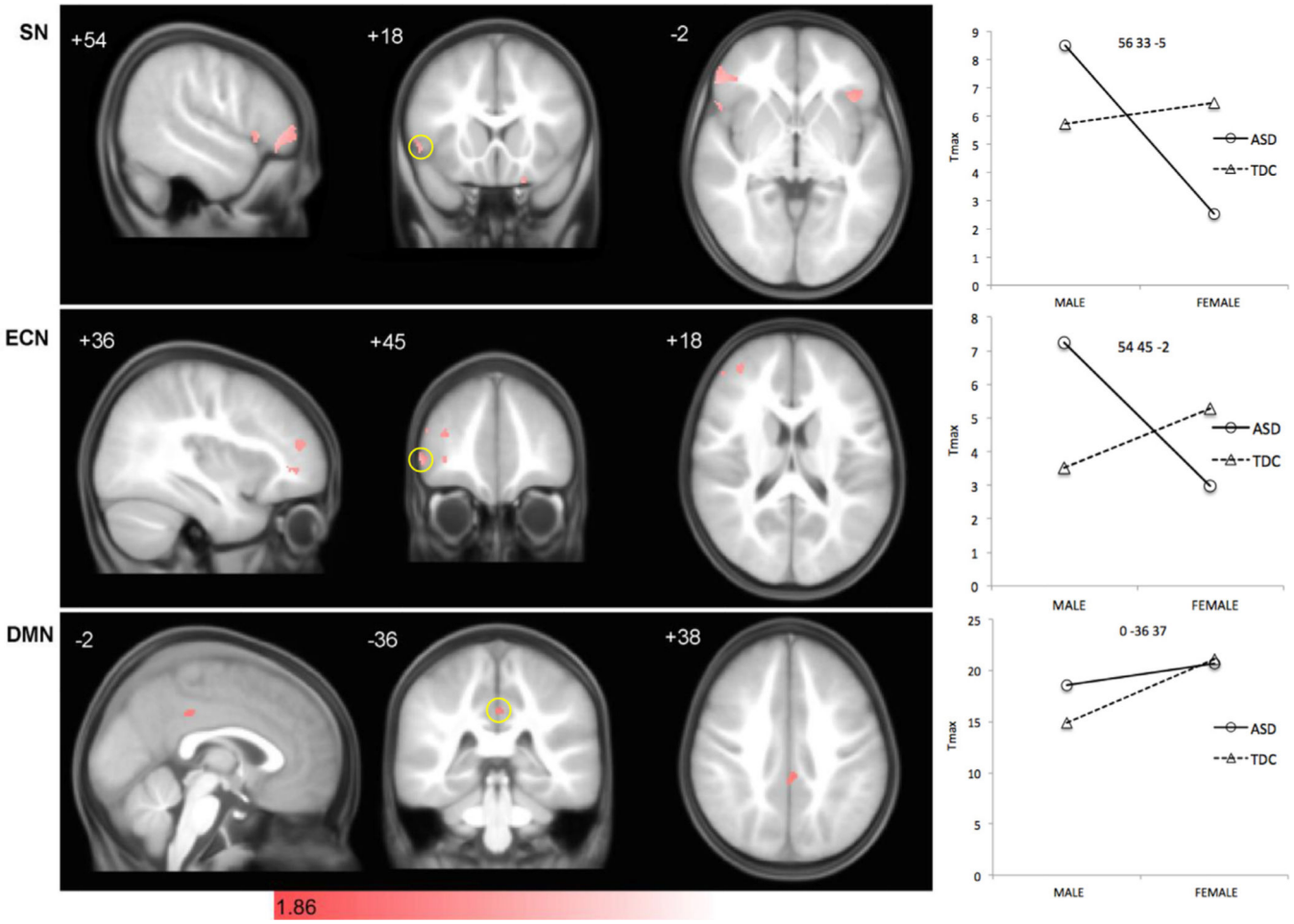

Fig. 5. Direct diagnosis by sex interactions in Salience, executive-control, and default mode networks in males and females.

Statistical parametric maps depict brain regions showing diagnosis-by-sex interactions in covariance with the seed hub for each network (pink). (Top) Salience Network interactions were seen in bilateral frontal operculum, right lateral prefrontal, and left orbitofrontal cortex (see also Supplemental Table 1). (Middle) DLPFC interactions effects were more distributed, showing covariance in multiple regions of right prefrontal cortex (see also Supplemental Table 1). (Bottom) In the Default Mode Network, a single node showed significant interaction effects in left posterior cingulate cortex. scMRI data are T-statistic maps ($p < 0.05$, of diagnostic group by sex interactions derived from SCNs at $p < 0.01$ FWE-corrected) displayed on the average anatomical template of all subjects. The left side of the image corresponds to the right side of the brain. $n = 122$ per group. Right panel depicts T-statistic magnitude for each subgroup at the Tmax centroid from the left panel. Respective coordinates are shown in each panel, corresponding to clusters highlighted by yellow circles on the coronal slice. FWE, family-wise error; ROI, region of interest; scMRI, structural covariance MRI; DLPFC, dorsolateral prefrontal cortex.

Table 1

Participant demographics.

	ASD Male (*n* = 61)	ASD Female (*n* = 61)	TD Male (*n* = 61)	TD Female (*n* = 61)
Age (Months)	36.49 (6.17)	38.67 (6.32)	36.75 (6.34)	38.42 (6.90)
IQ	65.76 (23.24)	66.09 (23.93)	102.72 (11.65)	108.58 (11.69)
ADOS CSS	7.68 (1.91)	7.42 (1.81)	–	–
ADOS SA-CSS	7.01 (1.71)	6.93 (1.65)	–	–
ADOS RRB-CSS	8.50 (1.53)	8.18 (1.55)	–	–

Note: Values are given as mean (standard deviation). ASD = Autism spectrum disorder, TD = non-autistic typically developing controls, ADOS = Autism Diagnostic Observation Schedule, CSS = calibrated severity score, SA-CSS = social affective calibrated severity score, RRB-CSS = restricted and repetitive behavior calibrated severity score.